Allosteric kinetics and equilibria of triligated, cross-linked hemoglobin

Mingdi Zhao,* Jie Jiang,* Michael Greene,‡ Mark E. Andracki,§ Scott A. Fowler,§ Joseph A. Walder,§ and Frank A. Ferrone*

*Department of Physics and Atmospheric Science, and ‡Biomedical Science and Engineering Institute, Drexel University, Philadelphia, Pennsylvania 19104; and §Department of Biochemistry, University of Iowa, Iowa City, Iowa 52242 USA

ABSTRACT Using modulated excitation, we have measured the forward and reverse rates of the allosteric transition between relaxed (R) and tense (T) quaternary structures for triply ligated hemoglobin (Hb), cross-linked between the α chains at Lys 99. Oxygen, carbon monoxide, and water were used as ligands and were studied in phosphate and low Cl^- bis-Tris buffers at neutral pH. Since the cross-link prohibits disproportionation, triply ligated aquomet Hb species with ferrous β chains were specifically isolated by isoelectric focusing. Modulated excitation provides rate pairs and therefore gives equilibrium constants between quaternary structures. To coordinate with that information, oxygen binding curves of fully ferrous and tri-aquomet Hb were also measured. L_3, the equilibrium constant between three liganded R and T structures, is determined by modulated excitation to be of order unity for O_2 or CO (1.1 to 1.5 for $3O_2$ and 0.7 for 3CO bound), while with three aquomet subunits it is much greater ($\geq$23). R $\rightarrow$ T conversion rates are similar to those found for HbA, with weak sensitivity to changes in L_3. The L_3 values from $Hb_{XL}O_2$ were used to obtain a unique allosteric decomposition of the ferrous O_2 binding curve in terms of K_T, K_R, and L_3. From these values and the O_2 binding curve of tri-aquomet Hb_{XL}, L_3 was calculated to be 2.7 for the tri-aquomet derivative. Consistency in L_3 values between equilibrium and modulated excitation data for tri-aquomet-Hb_{XL} can be achieved if the equilibrium constant for O_2 binding to the α chains is six times lower than that for binding to the β chains in the R state, while the cooperative properties remain homogeneous. The results are in quantitative agreement with other studies, and suggest that the principal effect of the cross-link is to decrease the R state and T state affinity of the α subunits with almost no change in the affinity of the β subunits, leaving the allosteric parameters L and c unchanged.

INTRODUCTION

In the attempt to find suitable blood substitutes, the notion of using pure acellular hemoglobin (Hb)[1] has been an attractive possibility for avoiding blood-borne disease and the necessity of blood typing. While Hb tetramers can deliver oxygen satisfactorily without being encased in some type of cell, a formidable problem that must be overcome is that the duration of a transfusion of acellular Hb is limited by the reversible dissociation of the tetramer into dimers, which are removed from circulation. Hb tetramers that are cross-linked to prevent dissociation (1, 2) avoid this problem while still providing a cooperative, functional oxygen delivery system.

Hb tetramers have been cross-linked at Lys 99α with lowered affinity and cooperativity similar to normal HbA (1–3). There has been much speculation as to the source of the lowered affinity. Chatterjee et al. (1) found that the increased p50 was due to the decrease in K_R with a possible small increase in L. Larsen et al. (4) used Raman spectroscopy of the cross-linked molecule to argue that the relaxed (R) state had become more "T-like" and hence had reduced affinity. Vandegriff et al. (5) found functional heterogeneity, and, using kinetic methods, concluded that cross-linking lowered the affinity for the last oxygen molecule sixfold for the α chains and twofold for the β chains.

Modulated excitation provides a powerful tool for investigating the allosteric properties of this cross-linked molecule. Modulated excitation methods use weak photodissociation to study the R $\rightarrow$ T conversion rates with three ligands bound (6). By observing the absorption spectra characteristic of the structure change, and tuning out the ligand rebinding rate, in most cases this provides both forward and reverse rates of structure change, even in the presence of rapid recombination rates, such as found with oxygen as a ligand. Since rate pairs are determined, the method provides a model independent measurement of the equilibrium between allosteric structures with three ligands. This can be advantageous in describing such changes as cross-linking produces. Although R and T structural endpoints are used, the method of modulated excitation is independent of the critical assumptions in the allosteric model, viz., that the change in quaternary structure is the predominant means by which affinity is changed, and that, without quaternary change, affinity remains constant. Modulated excitation does assume that there is a structure change that can be observed by known absorption spectra. This assumption has been recently strengthened by the demonstration that the fluorescence quenching of a DPG analogue follows this three-liganded spectral signature (7).

We report here the results of modulated excitation studies on cross-linked Hb. Since the tetramers do not dissociate, it is possible to isoelectrically focus partially oxidized samples to separate them by number of ligands, without disproportionation afterwards (8). Isoelectrically focused triferric derivatives with β ferrous subunits have been prepared and compared with ferrous cross-

Address reprint requests to F. A. Ferrone.

[1] *Abbreviations used in this paper:* DPG, 2,3 diphosphoglycerate; Hb, hemoglobin; MWC, Monod–Wyman–Changeux; R, relaxed; T, tense.

0006-3495/93/05/1520/13 $2.00

Biophys. J. © Biophysical Society
Volume 64 May 1993 1520–1532

linked Hb with 3CO or O_2 ligands. The modulated excitation results imply that the three-liganded T state is significantly populated. L_3, the ratio of T state to R state population with three ligands, is about unity for CO and O_2. For three aquomet ligands on ferric hemes, the T state is found to be dominant, and since k_{TR} is too small to be resolved clearly, even though k_{RT} can be determined unambiguously, the method can only place a lower limit on L_3.

As an alternate means of determining L_3 for the tri-aquomet derivative, binding curves were determined for that derivative and the fully ferrous cross-linked molecule. At this point, analysis requires a means of identifying the T state oxygen binding constant at the last ligation step of tri-aquomet Hb. We did this by equating it to the T state binding of the first oxygen binding step in fully ferrous Hb_{XL}. This explicitly invokes an allosteric model.

The values of the two determinations of L_3 differ by at least an order of magnitude. However, the differences can be reconciled by one assumption, viz., that the intrinsic binding constant for the α chains has been lowered sixfold by the cross-link without effect on the β chains or the allosteric mechanism. By analyzing the binding curve of the fully ferrous cross-linked derivative with explicit inequivalence of subunits, we are then able to interpret the binding curve of the aquomet derivative in a way consistent with the modulated excitation requirement of large L_3. While more complicated scenarios, including the possible breakdown of the allosteric model itself, are not excluded by the assumption of functional heterogeneity of the subunits, it is consistent with other work (5) and suggests that the cross-link may lower affinity by a relatively simple means.

MATERIALS AND METHODS

Hb was purified as described elsewhere and stored frozen (8). Isoelectric focusing produced ~80% β-ferrous of the triply oxidized molecules. When stock solutions were thawed, 2 mM sodium dithionite was added to reduce any methemoglobin present (except for tri-aquomet samples), and the sample was then immediately passed through a small preparative column (PD-10, 9 ml column of Sephadex G-25M [Pharmacia Fine Chemicals, Piscataway, NJ]) to remove dithionite and its products and to place Hb into the correct buffer. The column was eluted with either 0.15 M phosphate buffer, pH 7.0, or 0.05 M bis-Tris buffer, pH 7.0 (7–9 mM Cl^-), and the Hb was then concentrated to ~1 mM using microconcentrators (Centricon-30; Amicon Corp., Scientific Sys. Div., Danvers, MA). Samples so purified were used within 1 wk. Samples were sealed between coverslips in room air with a final Soret absorbance of near 1 OD. Soret absorption spectra were regularly monitored during the course of the experiments. Sample temperature during the experiment was regulated by a thermoelectric controller. Partially saturated HbO_2 samples were prepared by allowing room-equilibrated samples to be exposed to a wet nitrogen atmosphere for varied amounts of time in a refrigerated, nitrogen-purged glove chamber, where the samples were finally sealed. For oxygenation measurements, fully ferrous samples included a modification of the Hayashi reductase enzyme system in the proportions described by Sunshine et al. (9).

The modulation apparatus is that described by Martino and Ferrone (7). Three additional changes have been incorporated. First, the Ortec (EG&G, PAR; Trenton, NJ) lock-in amplifier has been replaced by an SR530 (Stanford Research Systems, Sunnyvale, CA) lock-in amplifier. Second, to retain high sensitivity through the lowered absorbance of the Soret band, a programmable high voltage supply was varied to keep the phototube DC anode current constant. This feedback was accomplished by computer control in a step-and-read fashion, giving the high voltage time to stabilize before a new reading is taken. Third, the acoustooptic modulator was replaced by an electrooptic modulator (Cambridge Research and Instrumentation, Cambridge, MA) with intrinsic feedback stabilization. Instead of feeding back against a DC reference, the feedback used a sine wave, thereby ensuring that the modulated signal was precisely sinusoidal and thus devoid of harmonics. Since the lock-in amplifier also uses linear mixing rather than square-wave mixing, there are no problems of higher harmonic response.

Modulated absorbance spectra were collected between 400 and 450 nm; excitation was accomplished by a modulated argon-pumped dye laser with emission at 573 nm. The level of excitation was monitored and kept <2% photolysis of the hemes. Because modulated excitation demands that only a small fraction of the sample be excited, the lower quantum yield of oxyhemoglobin is not a significant problem. Oxygen photolysis levels were typically ≤0.5%.

In modulated excitation, two types of measurement are performed that differ most fundamentally in the tuning of the detection system (6). In the first measurement, tuning is accomplished by setting the monochromators to 436.5 nm, an isosbestic of the R and T spectra, and adjusting the detection phase to bring the entire signal into the in-phase channel. Thus, the in-phase signal is contributed equally by R and T state populations, and the detection system is in tune with the result of excitation. The out-of-phase spectrum (rotated 90° from the in-phase spectrum) is, consequently, dominated by the spectrum arising from the change between R and T. A spectrum of the modulated species is measured at this phase, and excitation frequency, ω. Γ is used to denote the ratio of the out-of-phase R–T signal to the in-phase ligand-loss signal. This is the out-of-phase part of the ratio of molecules in the T structure to the total excited population. Γ is related to the kinetic processes that populate and depopulate the T state. For equivalent subunits,

$$\Gamma = \frac{\omega k_{RT}}{(k_{RT} + k_{TR} + k_T[X])^2 + \omega^2}. \tag{1a}$$

In this expression, the rate constants k_{RT}, k_{TR}, and k_T denote the rate of transition from R to T, from T to R, and the rate constant for ligand rebinding in the T state, respectively. $[X]$ denotes the concentration of free ligands (CO or O_2). These rates are defined to be those that occur with three ligands bound, which may differ from those at other ligation states, particularly in the case of the R–T rates. Eq. 1a peaks at a frequency ω^* equal to the sum of the rates ($k_{RT} + k_{TR} + k_T[X]$). The maximum of Γ, i.e., $\Gamma(\omega^*)$, is given by $k_{RT}/2(k_{RT} + k_{TR} + k_T[X])$. The product of ω^* and $\Gamma(\omega^*)$ will give $k_{RT}/2$. Separation of k_{TR} and $k_T[X]$ requires determination of the latter. This can be achieved by varying $[X]$. When $k_T[X]$ is small, as it is for CO binding, the maximum of Γ is directly related to L_3 ($\equiv k_{RT}/k_{TR}$), the allosteric equilibrium constant between R and T with three ligands.

If there is inequivalence in the binding or R $\rightarrow$ T conversion rates, the expression for Γ is more complicated, albeit straightforward. If the first harmonic oscillatory terms of the three liganded R and T states are denoted as R_α and T_α, and similarly for the β subunits, then Γ is calculated by evaluating the expression

$$\Gamma = -Im\left(\frac{T_\alpha + T_\beta}{R_\alpha + T_\alpha + R_\beta + T_\beta}\right), \tag{1b}$$

where Im denotes the imaginary part. It is worth noting that when this equation is evaluated, R state ligand binding kinetics are removed from the expression, and in particular, kinetic inequivalence in the R state per se has no effect on Γ (though kinetic T state equivalence can influence Γ via k_T.) If the simple form of Γ (Eq. 1a) is used to analyze data with inequivalence, instead of the correct Eq. 1b, the amount of allosteric conversion will be underestimated, and L_3 determined that way will be a lower limit to the subunit-averaged value of L_3.

The second measurement involves setting the detection monochromator to the laser wavelength, 573 nm, and tuning the phase so that the laser signal (rather than the observed population) is entirely "in-phase." This puts the detection system in phase with the source of the excitation (the laser), so that phase shifts show the system response relative to the excitation. In-phase and out-of-phase measurements are then recorded at a single wavelength (436.5 nm). The ratio of the out-of-phase to in-phase signal with this tuning is denoted than ϕ and is dominated by the ligand rebinding rate in the R state, but is only weakly affected by the kinetics of allosteric change and/or rebinding in the T state. For equivalent subunits, it can be shown (10) that

$$\tan\phi = \frac{\omega[\omega^2 + (k_T + k_{TR} + k_{RT})^2 + k_{RT}(k_R - k_T)]}{k_R\omega^2 + (k_T + k_{TR} + k_{RT})[k_T(k_R + k_{RT}) + k_R k_{TR}]}, \tag{2a}$$

where we have written k_R and k_T for $k_R[X]$ and $k_T[X]$ for compactness. (Note that $\tan\phi$ is a negative number. In practice, we will plot this as a sequence of positive numbers. This is formally equivalent to plotting $-\tan\phi$.) As ω becomes large, $\tan\phi \rightarrow -\omega/k_R[X]$. When $\tan\phi$ becomes proportional to ω, the ligand binding rate is just the inverse of the slope, and the values for R $\rightarrow$ T conversion do not enter that computation. If $\tan\phi$ is not proportional to ω, it is still strongly sensitive to R state ligand binding, but with observable contributions from the R $\rightarrow$ T conversion rates, and determination of k_R will depend on the determination of the other rates in the problem. Since k_{RT}, k_{TR}, and k_T are all set in the evaluation of Γ, fitting $\tan\phi$ to data involves variation of a single parameter. In the case of inequivalent rates of ligand binding to the subunits,

$$\tan\phi = \frac{Im(R_\alpha + R_\beta + T_\alpha + T_\beta)}{Re(R_\alpha + R_\beta + T_\alpha + T_\beta)}, \tag{2b}$$

in which Re and Im indicate the real and imaginary parts of the expression. Again, this expression is straightforward to evaluate given the rates.

Oxygenation experiments were performed on an apparatus of our own design in which complete spectra are gathered at randomly chosen values of pO_2, set by mass flow controllers and calibrated tanks of diluted oxygen. The sample itself is mounted in a Gill-type cell (11), in which oxygen is exchanged through a membrane that confines a thin Hb sample. By singular value decomposition (12), the spectral information can be reduced to simple binding curves. The method will be published in detail elsewhere.

RESULTS

Modulated excitation experiments were performed at 25°C at frequencies between 50 and 5,000 Hz. Cross-linked, fully ferrous Hb was studied by photolysis of the CO and O_2 derivatives. Although experiments on triferric derivatives were tried with CO and O_2 as the fourth ligand, the CO experiments proved unstable. Over the course of the several hours required to complete an experiment, the samples showed consistent autoreduction and traces of O_2. Attempts to remove the O_2 without reduction were unsuccessful. Thus, triferric derivatives were all studied by the photolysis of oxygen.

The method of modulated excitation depends on the correct quantitative identification of the observed spectral signal. Singular value decomposition (12) is a systematic way of reducing a set of spectra to principal components and effectively summarizing the spectra of a given experiment. Fig. 1 shows the principal in-phase (*a–c*) and out-of-phase spectra (*d–f*) for three complete experiments in which the remaining ligands were CO, O_2, and H_2O (met). For the triferric experiment, the photolyzed ligand was oxygen. The most representative component is the one drawn in filled circles; the second most representative spectrum is drawn with open circles. As can be seen, the major components were very well fit by the standard spectra consisting of: *a*) deoxy-minus-CO or deoxy-minus-O_2 difference spectra, *b*) deoxy RT difference spectra, and *c*) CO R–T difference spectra. The in-phase signals were dominated by the ligand rebinding and removal signal. The second most significant component (*open circles*) contributes very little to the in-phase spectra. 95% of the in-phase signal is described by the first component (*filled circles*) for the fully ferrous derivatives, and 90% for the triferric derivative. In the out-of-phase spectra, the first component represents ~80% of the ferrous derivatives and ~50% of the triferric derivatives. The second component is shown as the open circles. It is also well fit by the standards, though there is greater deviation in the case of the triferric experiments. The presence of higher order components most likely means that the tuning for setting the detection system is not perfect, as signified by the degree to which ligand-binding difference spectra appear in the out-of-phase channel. This can happen because of the smallness of the out-of-phase signal, ~20-fold smaller than the in-phase signal. (Since the spectra obtained here are difference spectra that are synchronous with the excitation, they do not represent differences that can arise because of long-term changes in the sample because of oxidation or reduction, for example.) For analysis of the R $\rightarrow$ T transition, the in-phase and out-of-phase spectra at each frequency were fit with the standards described above, and the coefficients of the standards were then used in the subsequent analysis.

Fig. 2 *a* shows Γ, the fraction of out-of-phase T state signal, as a function of excitation frequency ω for $Hb_{XL}CO$ in phosphate buffer. The curve is well fit by the simple description of Eq. 1a. The maximum of Γ is notably greater than experiments performed on Hb_ACO, which means a much greater fraction of molecules switch to the T structure. For Hb_A, k_T is small, i.e., $\sim 1.0 \times 10^5\ M^{-1}\ s^{-1}$. Bellelli et al. (12a) found $k_T[CO]$ also small in Hb_{XL}, viz., $1.5 \times 10^5\ M^{-1}\ s^{-1}$. This gives $k_{RT} = 2.9 \times 10^3\ s^{-1}$, and $k_{TR} = 4.3 \times 10^3\ s^{-1}$ by fitting to Eq. 1a. These values imply $L_3 = 0.70$. In Fig. 2 *b*, the rebinding kinetics of the fourth ligand can be determined by the tangent of absolute phase measured as a function of excitation frequency. The closeness of the curve to a straight line, particularly at higher frequencies, allows $k_R[CO]$ to be determined independent of values used to

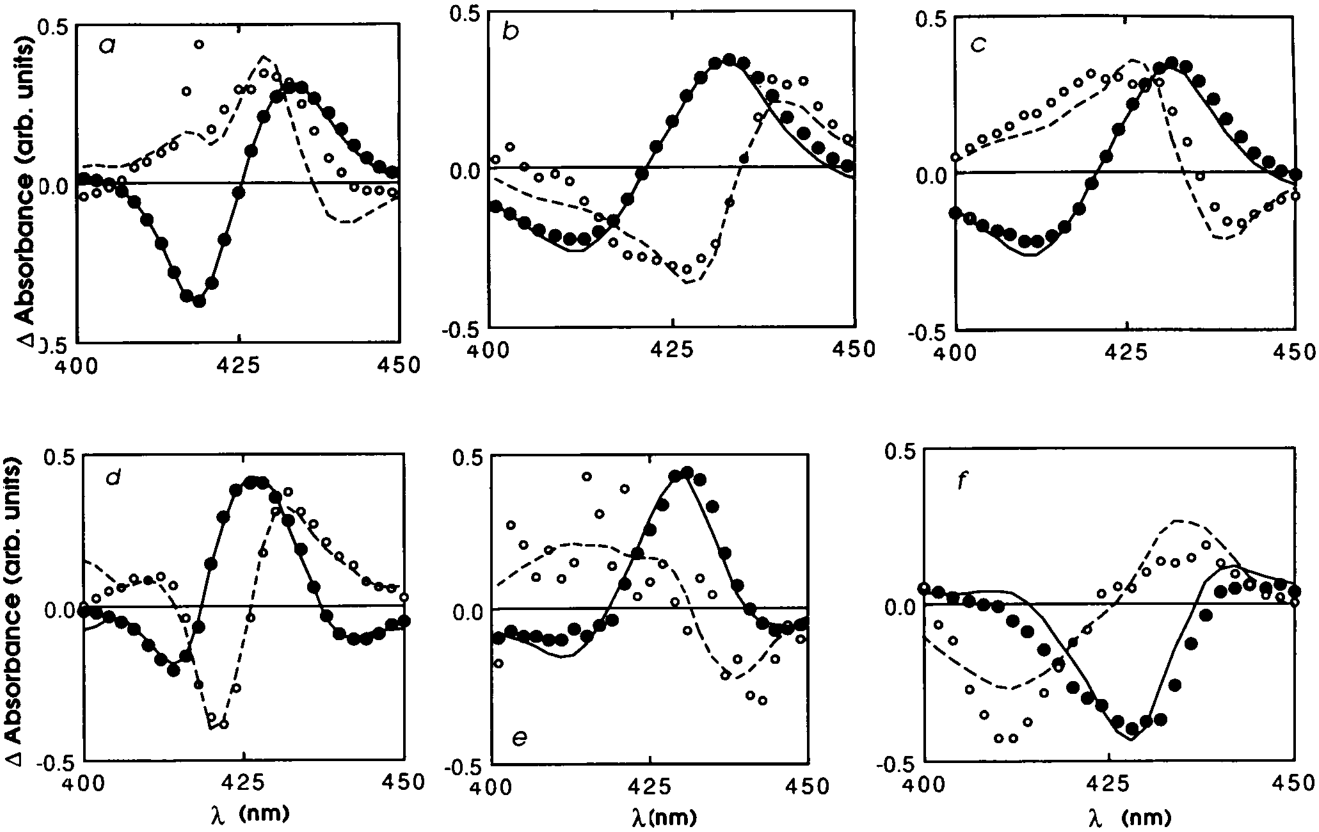

FIGURE 1 Principal spectra from modulated excitation experiments. *a* and *d* show experiments with photolysis of $Hb_{XL}CO$; *b* and *e* show photolysis of $Hb_{XL}O_2$; *c* and *f* show photolysis of oxygen bound to triferric aquomet Hb_{XL}. In each experiment, 10–20 spectra are collected: half are in phase with the excitation as measured at 436.5 nm (*a–c*); half are out of phase (*d–f*). In-phase and out-of-phase spectra are analyzed by singular value decomposition to obtain the principal components in each experiment. The most significant spectrum is shown as the filled circles; the second most significant spectrum is shown as the open circles. The spectra are fit, in turn, by standard spectra, and the fits provide the lines (*solid* or *broken*) shown in the figure. Standard spectra consist of ligand bound minus deoxy spectra plus a T-R difference spectrum obtained from the literature (30). In addition, for HbCO, a ligand-sensitive T-R difference spectrum is used (31). All Hb's are cross-linked, in pH 7 phosphate buffer. Although the spectra are shown normalized to the same amplitude, their contribution to the data set is drastically different. The following are the contributions for the first three components (only two have been plotted), relative to the in-phase spectra, taken as unity: (*a*) 1.00, 0.04, 0.02; (*b*) 1.00, 0.06, 0.005; (*c*) 1.00, 0.12, 0.03; (*d*) 0.041, 0.012, 0.005; (*e*) 0.047, 0.010, 0.008; and (*f*) 0.091, 0.047, 0.028. Absolute amplitude of the in-phase spectra is ~2 milli-OD. All out-of-phase spectra are shown magnified by a factor of 10. The quality of the fits indicates that the standard spectra provide a good representation of the entire data set.

fit Γ. This yields a rate of $3.7 \times 10^3\ s^{-1}$, which gives a rate constant $k_R = 3.7 \times 10^6\ M^{-1}\ s^{-1}$, assuming that the solution was fully saturated at 1 mM free CO. The curve shown is computed from Eq. 2a, and includes the parameters of the fit from Fig. 2 *a*, in addition to the rate constant k_R, to which tan ϕ is particularly sensitive.

Oxyhemoglobin samples were prepared in both bis-Tris (low Cl^-) and phosphate buffers. As discussed in Methods, while k_{RT} is uniquely determined, the value of k_{TR} depends on the determination of $k_T[O_2]$. This is done below for the tri-aquomet samples by variation of $[O_2]$, and the results are used throughout the analysis. To give an overview, however, all the oxygen photolysis results will be described qualitatively, and thereafter the numerical results and the assumptions used will be delineated. Γ is shown as a function of ω for $Hb_{XL}O_2$ in Fig. 3 *a* for phosphate buffer (*open squares*) and bis-Tris buffer (*filled circles*). The increase in Γ when phosphates are present means that the ratio $k_{RT}/(k_{TR} + k_T[O_2])$ has increased. This is to be expected if phosphates increase L_3 leaving $k_T[O_2]$ relatively unaffected. The maximum value of Γ (denoted $\Gamma(\omega^*)$) and the frequency at which the signal peaks, ω^*, are close to the values for CO. Since $k_{RT} = 2\omega^*\ \Gamma(\omega^*)$, it follows directly that k_{RT} is close to its value with CO ligands.

Fig. 3 *b* shows the tan ϕ as a function of frequency for O_2 binding to Hb_{XL} in phosphate and bis-Tris buffer. As expected, the rate of O_2 binding to Hb_{XL} (*open squares*) is faster than that for CO (Fig. 2 *b*), giving a lower tan ϕ at high frequencies. There is a slight dependence of the ligand binding kinetics on buffer, though the error bars of individual points overlap.

It is also interesting to compare these results with those obtained for Hb_A (13). Fig. 3 *c* shows that the tan ϕ for $Hb_{XL}O_2$ (*open squares*) is clearly higher than that of Hb_AO_2 (*filled triangles*). Both data sets are obtained in

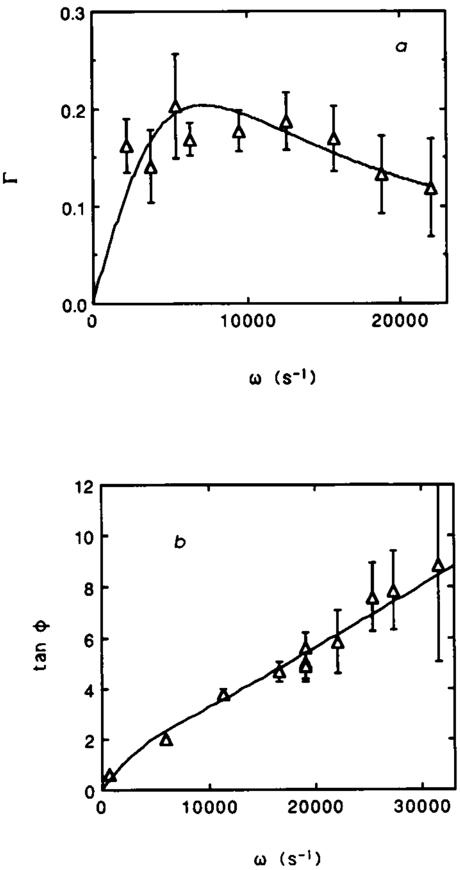

FIGURE 2 Modulated excitation of $Hb_{XL}CO$ in phosphate buffer. (*a*) Γ is shown as a function of excitation frequency, ω. Γ is the out-of-phase allosteric conversion, given by the size of the out-of-phase R–T spectrum (e.g., Fig. 1 *d*) normalized by the in-phase ligand binding spectrum (e.g., Fig. 1 *a*). Error bars are determined by the accuracy of the fit of the constituent spectra. (*b*) tan ϕ vs. excitation frequency ω. The phase angle is that between the out-of-phase and in-phase ligand-binding signals obtained when the system is in tune with the laser excitation. Since the asymptote of the tan ϕ curve is almost directly proportional to ω, determination of k_R depends little on the parameters used to describe Γ. For *a* and *b*, curves are drawn with the following parameters: $k_R = 3.7 \times 10^7\ M^{-1}\ s^{-1}$; $k_T = 1.5 \times 10^5\ M^{-1}\ s^{-1}$; $k_{RT} = 2.9 \times 10^3\ s^{-1}$; $k_{TR} = 4.2 \times 10^3\ s^{-1}$.

phosphate buffers. This implies that cross-linking has lowered the effective R state ligand binding rate.

Triferric (aquomet) samples were prepared with oxygen on the fourth (primarily β) heme, as described by Fowler et al. (8). Allosteric conversion in the presence and absence of inorganic phosphates is described by the fractional out-of-phase signal shown in Fig. 4 *a*. The magnitude of Γ is significantly greater than seen for $Hb_{XL}O_2$ in Fig. 3 *a*. The frequency at which the maximum Γ appears is also greater, and therefore k_{RT} has increased from its value for $Hb_{XL}O_2$. Unlike Fig. 3 *a*, where inorganic phosphates increased Γ, the effect (if any) of phosphates on the aquomet sample is to decrease Γ. The error bars in the aquomet modulation experiments are sufficient to allow a single curve to be drawn that is within the range of both data sets (with and without phosphate), although the best-fit parameters do show small differences. This is consistent with the data on fully ferrous Hb_{XL} (Fig. 3 *a*) if inorganic phosphates

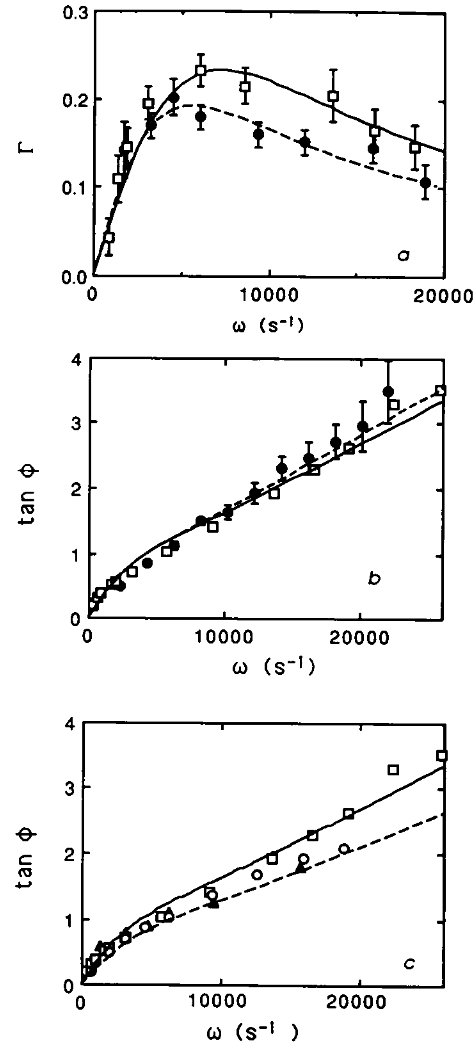

FIGURE 3 Modulated excitation of HbO_2. (*a*) Γ vs. excitation frequency ω. Γ is the out-of-phase allosteric conversion, given by the size of the R–T spectrum out of phase (e.g., Fig. 1 *e*) normalized by the in-phase ligand-binding spectrum (e.g., Fig. 1 *b*). Open squares are for $Hb_{XL}O_2$ in phosphate buffer, while filled circles are for bis-Tris. Phosphate buffer produces noticeably more allosteric conversion. The solid curve is the fit for phosphate buffer ($k_{RT} = 3.0 \times 10^3\ s^{-1}$; $k_{TR} = 2.0 \times 10^3\ s^{-1}$; $k_{R\alpha} = 2.3 \times 10^7\ M^{-1}\ s^{-1}$, $k_{R\beta} = 4.1 \times 10^7\ M^{-1}\ s^{-1}$; $k_{T\alpha} = 4.5 \times 10^6\ M^{-1}\ s^{-1}$ and $k_{T\beta} = 8.0 \times 10^6\ M^{-1}\ s^{-1}$), while the dashed curve is obtained in bis-Tris ($k_{RT} = 2.1 \times 10^3\ s^{-1}$; $k_{TR} = 2.0 \times 10^3\ s^{-1}$; $k_{R\alpha} = 1.9 \times 10^7\ M^{-1}\ s^{-1}$, $k_{R\beta} = 4.1 \times 10^7\ M^{-1}\ s^{-1}$; $k_{T\alpha} = 4.5 \times 10^6\ M^{-1}\ s^{-1}$ and $k_{T\beta} = 8.0 \times 10^6\ M^{-1}\ s^{-1}$). (*b*) tan ϕ vs. excitation frequency ω for Hb_{XL} in phosphate buffer (*open squares*) and bis-Tris buffer (*filled circles*). (*c*) Comparison of tan ϕ vs. excitation frequency ω for Hb_A and Hb_{XL} in phosphate buffer. Open squares are for $Hb_{XL}O_2$ (same data as in *b*); open circles are for tri-aquomet Hb_{XL}, from which oxygen is photolyzed and rebinds (also shown in Fig. 4 *b*; *filled triangles* are for Hb_AO_2 (13). Tan ϕ is larger for $Hb_{XL}O_2$, implying slower average ligand binding rates than Hb_AO_2. Tri-aquomet Hb_{XL} has essentially the same values as found for Hb_A. Thus we assume that the β chains, which represent the majority of the tri-aquomet data, are the same as both chains in Hb_A.

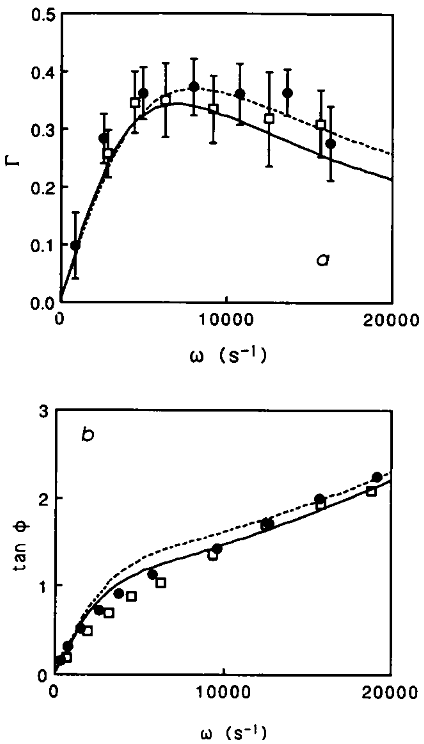

FIGURE 4 Modulated excitation of tri-aquometHb$_{XL}$O$_2$. (a) Γ is shown as a function of excitation frequency, ω. Γ is the out-of-phase allosteric conversion, given by the size of the R–T spectrum out of phase (e.g., Fig. 1 f) normalized by the in-phase ligand-binding spectrum (e.g., Fig. 1 c). Data for phosphate buffer are shown as the open squares; data for bis-Tris buffer are shown as filled circles. Error bars, which arise from the precision of the spectral fits, are large enough to suggest that there may be no effect upon the addition of inorganic phosphates. (b) tan ϕ vs. excitation frequency ω. Similarity in the data comparing the solid circles (bis-Tris) and empty squares (phosphate buffer) argues that the R state ligand binding kinetics do not change as the buffer is changed. For a and b, solid curves are for phosphate buffer, using the following parameters: $k_R = 4.1 \times 10^7\ M^{-1}\ s^{-1}$; $k_T = 8.0 \times 10^6\ M^{-1}\ s^{-1}$; $k_{RT} = 4.8 \times 10^3\ s^{-1}$; $k_{TR} = 100\ s^{-1}$. Dashed curves are for bis-Tris buffer, using the following parameters: $k_R = 4.1 \times 10^7\ M^{-1}\ s^{-1}$; $k_T = 8.0 \times 10^6\ M^{-1}\ s^{-1}$; $k_{RT} = 6.0 \times 10^3\ s^{-1}$; $k_{TR} = 10\ s^{-1}$.

primarily affect k_{TR}, and if the dominant escape path from T_3 in the aquomet sample is through ligand rebinding, i.e., if in that case $k_T[O_2] \gg k_{TR}$. This would mask changes in k_{TR}, keeping Γ about the same in spite of changes in L_3 due to phosphates.

The rate of oxygen binding to the aquomet derivative also showed very little sensitivity to the presence of inorganic phosphates, similar to our results for ferrous $Hb_{XL}O_2$. This is shown in the plot of tan ϕ as a function of ω (Fig. 4 b). However, the rate of oxygen binding to the aquomet derivatives is different from the binding rate to fully ferrous $Hb_{XL}O_2$. In Fig. 3 c, tan ϕ for oxygen binding to tri-aquomet Hb_{XL} is compared with ferrous Hb_{XL} and Hb_A. The high frequency parts of the tan ϕ curves for the aquomet cross-linked derivatives are significantly less than obtained for $Hb_{XL}O_2$, but they are almost identical to those obtained for Hb_AO_2. The difference between metHb_{XL} binding of O_2 and $Hb_{XL}O_2$ binding of O_2 must arise from the presence of ferrous α chains, since the ferrous hemes in tri-aquomet HbXL are contained in the β subunits. An attractive and simple hypothesis, therefore, is that the β subunit R state binding kinetics are unchanged by the cross-link, and that the rate of O_2 binding to Hb_A is fairly homogeneous despite differences in primary structure between α and β chains.

From Eq. 1a it is clear that fitting Γ will only give k_{RT} and the sum $k_{TR} + k_T[O_2]$. To separate k_T from k_{TR} for the triferric molecule, a series of experiments was conducted in which the oxygen partial pressure was varied. Because the samples are made by applying a few microliters to a coverglass, it is difficult to control the concentration of oxygen at values intermediate between room and zero oxygen pressure. Although it is easy to prepare a mixture of variously saturated solutions, it is hard to ensure the absence of oxygen exchange with the ambient gas in the glove box where the sample is prepared. Thus the final oxygen concentration was treated as a variable, rather than as a given. A series of partial saturated solutions was prepared, and both Γ and tan ϕ were measured as a function of ω. Fig. 5 shows the result of this experiment. From the changes in the tan ϕ data, it is evident that the partial pressure has been changed. Changes in Γ are also evident. Since the asymptotic slope of tan ϕ at high frequency is dominated by $k_R[O_2]$, that slope could be used to determine the various oxygen concentrations relative to atmospheric pressure. Rather than assume simple linearity, which requires that the asymptotic region has actually been reached, we fit both Γ and tan ϕ simultaneously to Eqs. 1 and 2, whereby the concentration-dependent rates could be uniquely determined. We deduce that, for oxygen binding to the β subunits, $k_R = 4.1 \times 10^7\ M^{-1}\ s^{-1}$ and $k_T = 8.0 \times 10^6\ M^{-1}\ s^{-1}$ in phosphate buffer (using air concentration as 0.26 mM O_2). k_{RT} is found to be $4.8 \times 10^3\ s^{-1}$.

This gives $k_T[O_2] = 2.1 \times 10^3\ s^{-1}$, and within the error limits accounts almost entirely for the sum of $k_{TR} + k_T[O_2]$ ($= 2.2 \times 10^3\ s^{-1}$), implying that the rate k_{TR} is essentially unresolved. The largest k_{TR} allowed by the estimate of uncertainty is $\sim$10% of $k_T[O_2]$. This uncertainty includes not only the random errors shown in Table 1 as errors in the fitting procedure, but also our estimate of systematic error, sample variation, and the like. Thus, it is possible for k_{TR} to be as large as $\sim$208 s^{-1}. With $k_{RT} = 4.8 \times 10^3\ s^{-1}$, this constrains $L_3^+ > 23$, where we adopt the notation that L_3 for the tri-ferric derivative is denoted L_3^+.

The tri-aquomet Γ values give $k_{RT} = 6.0 \times 10^3\ s^{-1}$ in bis-Tris buffer. Though Γ is systematically greater for bis-Tris than phosphate buffer in the tri-aquomet experiments, the uncertainty here is considerable. 10% uncertainty allows the plausible range for k_{RT} in bis-Tris to overlap the range of k_{RT} in phosphate buffer. In bis-Tris buffer, k_R was essentially the same as in phosphate buffer, and we shall assume the k_T is similarly insensi-

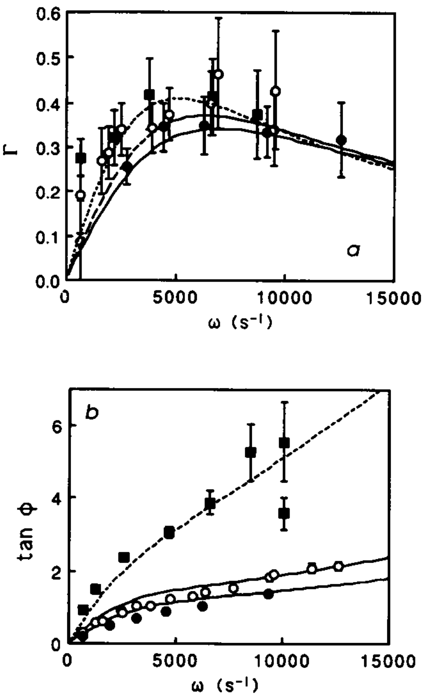

FIGURE 5 Modulated excitation of tri-aquomet $Hb_{XL}O_2$ in phosphate buffer for different concentrations of free O_2. (*a*) Γ vs. excitation frequency, ω. (*b*) tan φ vs. excitation frequency ω. All curves use the following parameters: $k_R = 4.1 \times 10^7\ M^{-1}\ s^{-1}$; $k_T = 8.0 \times 10^6\ M^{-1}\ s^{-1}$; $k_{RT} = 4.8 \times 10^3\ s^{-1}$; $k_{TR} = 100\ s^{-1}$. Decreasing the free ligand concentration has an enormous effect on tan φ but its effect is much smaller on Γ.

tive to the presence of inorganic phosphates. Setting $k_T[O_2] = 2.1 \times 10^3\ s^{-1}$ means k_{TR} is highly uncertain for bis-Tris buffer, as for phosphate. Thus, as a conservative estimate, we shall take $L_3^+ > 23$ with and without phosphates.

The ligand binding rates determined for the triferric molecule would be expected to apply to the fully ferrous Hb as well. Returning to the tan φ data for fully ferrous $Hb_{XL}O_2$ shown in Fig. 3 *b*, we see that this is not the case. The k_R determined for the triferric Hb_{XL} will give a tan φ much smaller than observed, as seen by comparing the open circles and open squares in Fig. 3 *c*. Since the triferric molecules are predominantly β-ferrous, the differences may be explained by heterogeneity in ligand binding kinetics. In such a case, the asymptotic slope of a tan φ curve is related to the mean of the rates. We set the triferric value for k_R equal to that for the β subunits in $Hb_{XL}O_2$ and fit the data for $Hb_{XL}O_2$ of Fig. 3 to Eqs. 1b and 2b to yield $k_{R\alpha} = 2.3 \times 10^7\ M^{-1}\ s^{-1}$ in phosphate buffer, and $1.9 \times 10^7\ M^{-1}\ s^{-1}$ in bis-Tris. From Fig. 3 *a* and Eq. 1a we found $k_{RT} = 3.0 \times 10^3\ s^{-1}$, and this is unchanged with inequivalence of binding kinetics.

Given inequivalence in rate of O_2 binding to the R state, it is plausible to expect inequivalence in the T state as well. From the triferric data a value of $k_{T\beta}$ was obtained. To complete the analysis of the ferrous Hb_{XL} data requires a value for $k_{T\alpha}$. We assume that the T state rates are heterogeneous in the same proportion as the R state rates, i.e., $k_{T\alpha}/k_{T\beta} = k_{R\alpha}/k_{R\beta} = 0.57$. This requires that $k_{T\alpha} = 4.5 \times 10^6\ M^{-1}\ s^{-1}$, and therefore $k_{TR} = 2.0 \times 10^3\ s^{-1}$. So long as the rate ratio is not dramatically different, the effects on the allosteric kinetics will be small. For example, if the T state oxygen-binding rates are equal for both subunits, $k_{TR} = 1.5 \times 10^3\ s^{-1}$. Thus, k_{TR} is not highly sensitive to this assumption that the T state inequivalence is proportional to that which we find in the R state. This then specifies the rates for $Hb_{XL}O_2$ in phosphate buffer. We find $k_{RT} = 3.0 \times 10^3\ s^{-1}$ and $k_{TR} = 2.0 \times 10^3\ s^{-1}$, with $L_3 = 1.5$. These are precisely the values obtained in Hb_AO_2.

Finally, we turn to $Hb_{XL}O_2$ in bis-Tris buffer. From the experiments in Figs. 3 *b* and 4 *b*, the R state oxygen-binding rate constant is essentially independent of phosphates. With the assumption that the oxygen-binding rate in the T state is likewise phosphate independent, $k_{T\alpha}$ and $k_{T\beta}$ can be assigned in bis-Tris buffer, and the R–T rates thereby resolved. We find $k_{RT} = 2.2 \times 10^3\ s^{-1}$ and $k_{TR} = 2.0 \times 10^3\ s^{-1}$, with $L_3 = 1.1$. The results are summarized in Table 1.

Because the modulated excitation data provided only an upper bound for L_3, an equilibrium binding curve for triferric Hb_{XL} was also measured. A noncooperative curve is expected, the binding curve of which is given by

$$Y = \frac{K_4^+[O_2]}{1 + K_4^+[O_2]}, \tag{3}$$

where the effective equilibrium constant K_4^+ is given by

$$K_4^+ = \frac{K_R + L_3^+ K_T}{1 + L_3^+} = K_R \frac{1 + L_3^+ c}{1 + L_3^+}. \tag{4}$$

Since the triferric species has essentially only β subunits available for binding, the equilibrium constants measured this way are subunit specific. Note that c in Eq. 4 refers to the ratio of equilibrium constants for oxygen binding to the β subunits and does not refer to the ratio of binding constants of the ferric subunits. Assuming that the oxygen affinity of a given subunit does not depend on the nature of the ligands on the other subunits but only on the quaternary structure, and assuming the subunits bind with equivalent affinity, the binding constants K_R and K_T in Eq. 4 can be determined by measuring the oxygen binding curve for the fully ferrous derivative. Fig. 6 shows a Hill plot of both the fully ferrous cross-linked Hb (*filled circles*) and the triferric aquomet derivative (*open circles*), taken in phosphate buffer at 11°C. A cooperative Hill plot has asymptotes for which the intercepts with the log $p = 0$ axis are log K_R and log K_T. The triferric derivative displays a linear Hill plot, which lies between the asymptotes for K_R and K_T. This is expected as a consequence of having a mixture of R and T state molecules, and directly suggests some conversion to the T state with three aquomet ligands. Small sample

TABLE 1 Allosteric rates and equilibria (25°C)

Ligand	Buffer*	k_R α	k_R β	k_T α	k_T β	k_{RT}	k_{TR}	L_3
		$M^{-1}s^{-1} \times 10^{-6}$		$M^{-1}s^{-1} \times 10^{-6}$		$s^{-1} \times 10^{-3}$	$s^{-1} \times 10^{-3}$	
Hb^{3+}_{XL}								
O_2‡	P	-	41 ± 1	-	8.0 ± 0.1	4.8 ± 0.1	≤0.2	≥23
O_2	B	-	41 ± 1	-	8.0 ± 0.1§	6.0 ± 0.7	≤0.2	≥23
Hb_{XL}								
CO	P	3.7 ± 0.6		0.1		2.9 ± 0.6	4.2 ± 0.5	0.70
O_2	P	23 ± 1	41 ± 1	4.5 ± 0.2‖	8.0 ± 0.1§	3.0 ± 0.1	2.0 ± 0.4	1.5
O_2	B	19 ± 1	41 ± 1	4.5 ± 0.2‖	8.0 ± 0.1§	2.2 ± 0.2	2.0 ± 0.3	1.1
Hb_A								
CO¶	P	6.0		0.1		1.5	3.9	0.38
CO**	B	6.5		0.1		3.4	21.0	0.16
O_2¶	P	40		5.6		3.0	2.0	1.5

Error estimates are based on increasing χ^2 by 1 while holding other parameters fixed. In computing χ^2, the standard error for each point was obtained by evaluation of the noise level in each experiment. These are the random errors of each experiment. We anticipate that other sources of error lie in the 10% range for most parameters.

* P = 0.15 M phosphate, B = bis-Tris, with 7–9 mM Cl^-.

‡ For three aquomet ligands, the photolyzed ligand was O_2, and is selected to be on the β subunits by isoelectric focusing (8).

§ Set equal to the metHb_{XL} phosphate value.

‖ Determined by assuming the same ratio between α and β for k_T as for k_R.

¶ Data from Zhang et al. (13). For Hb_AO_2, the solubility of O_2 in water was taken as 1 mM rather than 1.25 mM. Hence, the original rate constant has been reduced by a factor of 1.25.

** Data from Martino and Ferrone (7).

drift, mainly due to methemoglobin formation, accounted for no more than 1.3%/h, and is corrected out of the analysis (since the sequence of pressures is not monotonic).

While it is possible to describe a binding curve in terms of K_R, K_T, and L_0, it is difficult to obtain a unique decomposition since the values of K_R and L_0 are highly correlated. Fitting the fully ferrous oxygenation data to an unconstrained MWC model gives $K_T = 0.081 \pm 0.03$ mm Hg^{-1}, $K_R = 13 \pm 12$ mm Hg^{-1}, and $L_0 = 5 (\pm 19) \times 10^7$. K_R and L_0 have large uncertainties, as expected. These parameters gave an $L_3 = 12$, with considerable uncertainty (±56).

To avoid these problems, we adopted the following strategy. L_3 for oxygen binding is determined by modulated excitation, and so the MWC equation for the fractional oxygen saturation Y (14) was rewritten in terms of L_3 instead of L_0, and then L_3 was set as a constant in the fit. This left only K_R and K_T as free parameters. The equilibrium data of the fully ferrous derivative was fit to obtain these parameters. Fixing $L_3 = 1.5$, the fit to the ferrous binding curve gives $K_T = 0.077 \pm 0.03$ mm Hg^{-1} and $K_R = 2.2 \pm 0.3$ mm Hg^{-1} so that $c = 0.04$. The fit is indistinguishable from the unconstrained, three-parameter fit.

These parameters were then used in analyzing the aquomet derivative to give L_3^+. That derivative had a $K_4^+ = 0.55 \pm 0.02$ mm Hg^{-1}, which then, using Eq. 4, gives an $L_3^+ = 2.7 \pm 0.7$. This clearly depends on the initial setting of L_3 for the ferrous data. If we fixed $L_3 = 5.0$ instead of 1.5, then the L_3^+ becomes 11.3 (±0.3) instead of 5.4. (Fixing $L_3 = 5$ also gives $K_T = 0.080$ mm Hg^{-1}, which is almost unchanged, and $K_R = 5.9$ mm Hg^{-1}).

The equilibrium binding and modulated excitation determinations of L_3^+ differ substantially (2.7 and >23, respectively), suggesting that some assumption has broken down.[2] Since we have already observed kinetic heterogeneity in the ligand binding rates k_R, it is plausible that the subunit affinity is also heterogeneous. For simplicity, let us assume that the subunit heterogeneity occurs solely in the binding affinity for the R state, and that the allosteric parameter c (and therefore L_3) is the same for α and β chains. This, of course, requires heterogeneity in the T state affinity, in proportion to that in the R state.

$K_{R\alpha(\beta)}$ will denote the R state affinity of the α or β subunits. Consistent and good-quality fits are obtained with $c = 0.015$, $K_{R\beta} = 9.8$ mm Hg^{-1}, and $K_{R\alpha} = 1.7$ mm Hg^{-1} using our results that $K_4^+ = 0.55$ mm Hg^{-1}, $L_3^+ = 23$, and $L_3 = 1.5$. The ratio $K_{R\beta}/K_{R\alpha} = 5.8$. The solid curve in Fig. 6 is drawn with these parameters. This, of course, does not prove that subunit inequivalence is the source of the differences in equilibrium and modulation results,[3] but the similarity to the data of others (see be-

[2] The difference in temperature of the equilibrium and kinetic data is not likely to be significant here. Modulated excitation data on HbA find L_3 independent of temperature (13), while the work of Bellelli et al. (12*a*), in which the binding curve was observed over a wide temperature range, argues that adjusting the data to a common temperature will, if anything, increase the differences observed.

[3] It is also possible that the discrepancy in L_3 values originates in the presence of cooperative binding within the T state. K_T determined from

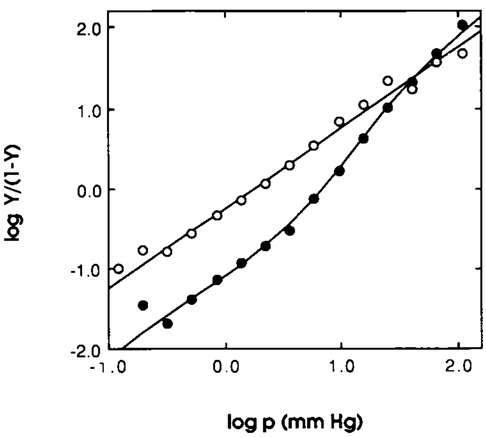

FIGURE 6 Hill plot for oxygen binding to fully ferrous Hb_{XL} (*filled circles*), and tri-aquomet Hb_{XL} (*open circles*) in phosphate buffer. Y is the fractional oxygen saturation. The tri-aquomet curve is a straight line that lies between the asymptotes of the fully ferrous sample, indicative of some degree of mixing of R- and T state affinities. By fitting the fully ferrous oxygenation data to an unconstrained MWC model, we obtained $K_T = 0.081 \pm 0.03$ mm Hg^{-1}, $K_R = 13 \pm 12$ mm Hg^{-1}, and $L_0 = 5\ (\pm 19) \times 10^7$. The equation for Y was rewritten in terms of L_3 instead of L_0, and L_3 then set constant. With $L_3 = 1.5$ (cf. Table 1), $K_T = 0.077 \pm 0.03$ mm Hg^{-1} and $K_R = 1.8 \pm 0.3$ mm Hg^{-1}. The fit is indistinguishable from the unconstrained, three-parameter fit. K_R and K_T are used in analyzing the aquomet derivative to give L_3^+ (cf. Eq. 3). The triferric derivative is characterized by a single affinity constant, $K_4^+ = 0.55 \pm 0.02$ mm Hg^{-1}. Using Eqs. 2 and 3, these data imply $L_3^+ = 2.7 \pm 0.7$. This disagrees with the limit set by modulated excitation experiments ($L_3^+ > 23$), but the discrepancy can be rectified by the assuming that the subunits have different oxygen affinities. The curve in the figure is drawn using a model in which the subunit affinities differ, but cooperativity operates by a single mechanism. Parameters are $c = 0.015$, $L_3^+ = 23$, $L_3 = 1.5$, $K_{R\beta} = 9.8$ mm Hg^{-1}, and $K_{R\alpha} = 1.7$ mm Hg^{-1}. The binding curve generated by these parameters is extremely close to the fit using a simple MWC formulation; both curves fit the data well within its precision.

low) strengthens that hypothesis. The value of 23 for L_3^+ is a lower limit. Enlarging this value increases $K_{R\beta}$ but does little to $K_{R\alpha}$.

DISCUSSION

Allosteric kinetics

The presence of the cross-link, which is formed in the T structure, might be expected to steer the allosteric $R \rightarrow T$ transition and so enhance its rate. This expectation is borne out in the $R_0 \rightarrow T_0$ transition (5), which is about six times faster due to the cross-link, and in the $R_3 \rightarrow T_3$ for CO, which is about two times faster. For HbO_2 in phosphate buffers the rate of the $R_3 \rightarrow T_3$ transition does not appear to be affected by the cross-link.

The effect on the $R \rightarrow T$ rate of additional ligands can be systematically described by plotting the log of the rate as a function of the log of the equilibrium constant, as is done for linear free-energy relationships (15). Fig. 7 shows the dependence of the $R \rightarrow T$ rates on the equilibrium constant L_n (where n is the number of ligands) for Hb_{XL} (*filled circles*) and Hb_A (*open circles*) in 0.1 M phosphate buffers or 0.1 M Cl^- tris. (Cl^- and phosphate buffers have similar effects on the allosteric equilibrium [14].) This viewpoint is supported by the degree to which the Cl^- data (*open circle with the error bars*) follows the same line as the phosphate data (*remaining open circles*). It is interesting that the cross-link has sensitivity to the rate constant k_{RT} similar to the change in equilibrium constant L_n, but consistently more rapid rates. This might indicate that while some steering by the

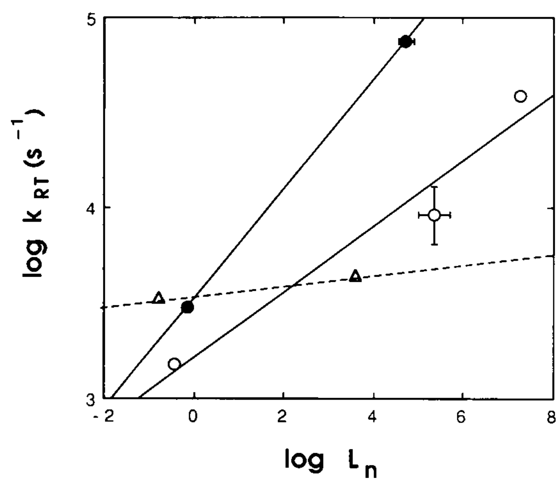

FIGURE 7 The dependence of the $R \rightarrow T$ rates on the equilibrium constant L for Hb_{XL} (*filled circles*) and Hb_A (*open circles* and *triangles*) with CO as a ligand. Circles show phosphate buffer; the circle showing x and y error bars is for 0.1 M Cl^- buffer; triangles are for Hb_A in <0.01 M Cl^- buffer. Error bars represent the range of averaged determinations of the given parameter measured by different investigators; error bars from the modulated excitation experiments are smaller than the symbols in the figure. The triliganded point for Hb_ACO in low Cl^- is taken from reference 7; the triliganded point for Hb_ACO in phosphates is taken from reference 13. The triliganded point for $Hb_{XL}CO$ is the phosphate buffer data taken from this study. The rates for zero-liganded Hb in 0.1 M Cl^- are taken from references 5 and 18; in phosphate buffer they are from references 16–18; in low Cl they are from reference 32. The L_0 values for Hb_{XL} are taken directly from reference 5 or by using the analysis in this paper, which gives values of L_3 and c. The L_0 values for Hb_A are taken from reference 5; from our analysis as above for Hb_{XL}; and from Ackers and Johnson (33). The rates for all three equilibrium measurements are the same, and the variation in L_0 is taken as a measure of uncertainty. The L_0 value for Marden's lower Cl^- conditions is taken from Imai (34); the L_0 value for phosphate is taken from an analysis (31) of the data of Imai and Yonetani (35). The best-fit slope through the cross-linked data (*filled circles*) is 0.30; the best-fit slope through the Hb_A data (*open circles*) is 0.18; the line through the triangles (Hb_A, low Cl^-) has a slope of 0.025.

the ferrous heme binding curves is dominated by the binding of the first ligand, whereas the triferric derivative is sensitive to the fourth ligand alone. Hence, in Eq. 4, the use of the K_T from the ferrous binding curve represents the assumption of full conformity with the MWC model. If this variation in ligand affinity is uniformly distributed, each subsequent ligand should bind to the T state with 1.8 times the affinity of its predecessor. In studies on ligand binding to HbA crystals in the T state, however, no cooperativity is observed. (29)

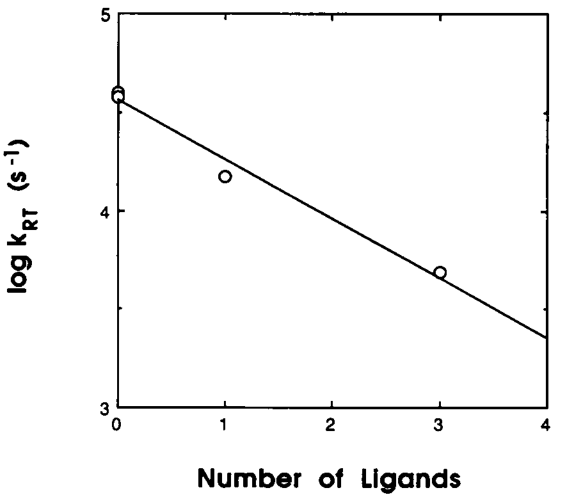

FIGURE 8 Correlation of the R → T rate and number of ligands. Zero ligand data for phosphate buffer is taken from Hofrichter et al. (17) and Cho and Hopfield (16). Single ligand data is HbA with fluoride bound to a single heme (16); three-liganded data is for aquo-met Hb_{XL}, taken from this paper. The slope is −0.30. To compare with Fig. 7, note that the equilibrium constants between structure with n ligands, L_n, is given by $L_n = L_0c^n$, so that log L_n is proportional to n log c.

cross-link occurs, the variation of rate has a connection to the allosteric mechanism, which is largely unchanged.

For comparison, data on lower Cl^- concentrations (<0.01 M) for Hb_A are also shown as the triangles. Though the rate of structure change without ligands is faster with effectors present, the reverse is true when three ligands are bound.

The data on metHb can be examined in a similar fashion. Since L_n, the equilibrium constants between structure with n ligands, is equal to L_0c^n, then $\log L_n = \log L_0 + n \log c$. Therefore, log L_n is proportional to n. The data from this work measure $R_3 \rightarrow T_3$ rates with aquomet ligands; a number of others have measured $R_0 \rightarrow T_0$ kinetics in phosphate buffer (16–18). Cho and Hopfield (16) also measured $R_1 \rightarrow T_1$ rates for high-spin, single-met molecules. Although the three-liganded data shown have been taken on cross-linked Hb, while the other points are on Hb_A, the $R_3 \rightarrow T_3$ rate for oxygen bound is identical for Hb_A and Hb_{XL}, as noted above. The resulting graph is shown in Fig. 8 and exhibits very good correlation. The slope here must be multiplied by log c(met), which is <0, in order to compare it quantitatively with the slopes shown in Fig. 7. The data of Fig. 8 provide the first direct support for the conjecture of Sawicki and Gibson (19) that the rate of structure change decreases by a constant factor for each additional ligand.

Equilibrium results

Allosteric equilibrium

Modulated excitation measurements provide a particularly precise way to determine L_3. Both Hb_A and Hb_{XL} have $L_3 > 1$, so that the switch in quaternary structures occurs after three ligands have bound. This is significantly different from the switchpoint value of 2.3 deduced from equilibrium binding studies (3), and the difference can be important in interpreting measurements on the binding of the last ligand, which will exhibit a mixture of R and T properties.

When the liganded subunits are aquomet, the allosteric equilibrium is substantially altered. Cooperativity is particularly affected in high spin derivatives. Szabo and Karplus (20) analyzed early work on metHb hybrids, concluding that fluoromet Hb_A had a value of c that is 2.4 times larger than the c for cyanometHb and ~5.7 times larger than azido-metHb. In agreement with prior findings, more recent experiments on partially oxidized Hb_A found a value for c for the fluoromet derivative that is 3.5 times that of the cyanmet derivative (21, 22). Analysis of an ensemble of binding curves of varied fractions of ferric material led Marden et al. (21, 22) to conclude that the L_3^+ for aquomet Hb should be ~11 near neutral pH, in bis-Tris buffer with 0.1 M Cl^-. This is in excellent agreement with our results, given the differences in conditions, and supports our observations that $L_3^+ \gg L_3$ in Hb_{XL}. This further strengthens the contention that cooperativity functions in the same way in the cross-linked derivative.

Ligand-binding equilibrium

Cross-linked Hb shows cooperativity but reduction in oxygen affinity. Initial analysis of equilibrium binding curves for Hb_{XL} reported a 3.7-fold decrease in the T structure binding constant compared with Hb_A, and possible shift in the allosteric equilibrium constant L_0 (1). However, it is generally possible to increase or decrease L_0 and K_R in tandem over a considerable range with little discernible effect on the ability of the theoretical curve to represent the equilibrium data. A subsequent study of Hb_{XL} binding curves (3) concluded that the cross-link decreased the binding constant for the first ligand (and thus K_T) by a factor of 2.1.

Vandegriff et al. (3) have recently attempted to determine the fourth ligand binding constant by kinetic means. This avoids various experimental difficulties that attend to equilibrium measurements in the limit of high saturation (23). Kinetic data were fit to two exponentials, and the subunits were identified by noting which relaxation changed upon addition of pMB, which is known to bind to the β subunits. They concluded that the subunits had different affinities, with binding constants of 1.2 and 0.37 mm Hg^{-1} for β and α chains, respectively.

Clearly, the determination depends on the correct resolution of kinetic data. On the basis of model-independent modulated excitation results, there will be a mixture of R and T state molecules in any partial photolysis experiment, creating multiple exponential relaxations. Given the mixture of allosteric species, it is doubtful that the addition of pMB will affect only the β chains as intended. There is evidence for a quaternary sensitivity of the β93 region, implying that perturbations induced there will affect the allosteric equilibrium, and so change the relaxation kinetics by affecting the degree of R and T mixing (14). In addition, the use of 20% photolysis in that work further complicates analysis by incorporating significant doubly liganded species.

If, despite the difficulties described above, the kinetic methods provide reasonable estimates for the effective binding constants for the last ligand, we can use the L_3 values obtained in this study to resolve the R state contributions. Thus we would interpret Vandegriff et al.'s data as giving an R state affinity of 2.8 and 0.52 mm Hg^{-1} for β and α subunits in the cross-linked tetramer. Our data yield 9.8 and 1.7 mm Hg^{-1} for β and α subunits. Differences between the two determinations may also arise from solution conditions, since our work is in phosphate buffer at pH 7 while that of Vandegriff et al. is in 0.1 M Cl bis-Tris at pH 7.5. The differences in conditions will not alleviate the difficulties of interpretation of the pulse kinetic data, however, for we have observed (unpublished results) for Hb_A that there is still a substantial conversion to the T state at 0.1 M Cl, pH 7.4 Tris. Interestingly, the subunit-averaged binding constant determined kinetically does agree with that found by equilibrium methods (5). Our effective binding constant for the last oxygen in Hb_{XL} is 1.2 mm Hg^{-1} when the subunits are appropriately averaged, in very good agreement with 1.5 mm Hg^{-1} of Vandegriff et al. The ratio of subunit affinities $K_{R\beta}/K_{R\alpha}$ is also quite similar, viz., 5.4 for the previous work versus 5.8 for this work.

If both subunits of Hb_A are equivalent and have the same affinity as found in this study for the β subunits of Hb_{XL}, then K_4 would be 4.0 mm Hg^{-1} for Hb_A. This is well within the range of accepted values. Philo and Lary (24) obtained 4.8 mm Hg^{-1} by kinetic methods. Using equilibrium methods, Chu et al. (25) got 5.2 mm Hg^{-1}, while Mills et al. (26) obtained 4.7 mm Hg^{-1}. Vandegriff et al. (5) determined K_4 for Hb_A to lie between 7.6 (equilibrium methods) and 5.9 mm Hg^{-1} (kinetic methods), while Chatterjee et al. (1) obtained 1.4 mm Hg^{-1}. It is thus plausible that the only effect of the cross-link is to decrease the intrinsic ligand affinity of the α subunit, leaving the β subunit affinity and the cooperative mechanism intact.

The last comment warrants elaboration. The cooperative mechanism in Hb entails the reduction of affinity with change in quaternary structure by diminishing the energy usually available for the iron ligand bond. The decrease in energy represents energy stored in some part of the molecule. If that energy is the same with and without cross-linking, then the ratio of T state to R state affinity will be the same, irrespective of the initial ligand affinity.

If the cooperative mechanism is left intact, the ratio of K_T/K_R is the same for both subunits. A reduction in α chain affinity by a factor of 5.8, as seen in these data, implies a change in average K_T by a factor of 1.7, very close to the factor of 2.1 observed by Vandegriff et al. (5). This supports the idea that the allosteric constant c has not been changed, i.e., that cooperativity works in essentially the same way with the cross-link present.

We have been able to describe the allosteric behavior of triply ligated Hb_{XL} by the assumption that both subunits function allosterically equivalently. With that assumption, the allosteric properties for HbO_2 are identical with and without the cross-link: k_{RT} and k_{TR}, and thus L_3, are the same. The reduced ligand affinity can be completely described by a single change, viz., reduction of the α subunit affinity. This does not exclude more complicated mechanisms in which the allosteric properties also differ for different chains. However, the addition of extra parameters does not seem required by these data.

It is worth noting that another simple model is excluded by known data. It might be tempting to assume that cross-linking has affected only K_R, making the subunit R state affinities different, but has left K_T unchanged and homogeneous. This is directly contradicted by the observations that the binding constant for the first ligand has changed with the cross-link.

Structural considerations

It is interesting to think of the deoxy α heme pocket as having been in some way distorted in the process of cross-linking. By opposing this distortion, ligation would result in a weakened iron–ligand bond. Such a distortion could still be irrelevant to the allosteric performance of the molecule for either of two reasons. One reason is that allosteric and cross-link–induced distortions could affect different coordinates. For example, suppose the iron–heme plane distance is a critical determinant of affinity. Cross-linking could pull the proximal histidine in one direction, while the cooperative mechanism produces a pull in a perpendicular direction. Pulling in either direction constrains the ease with which the iron enters the plane. Alternatively, the distortion may remain in the "elastic limit" so that the allosteric and cross-linked reduction in affinity can be simply superimposed.

Chatterjee et al. (1) found the T state x-ray structure essentially the same as that of Hb_A, while a change in Bohr effect was attributed to an R state pK change. Larsen et al. (4) studied the behavior of Hb_{XL} by resonance Raman scattering. They found that the low frequency iron–histidine stretching frequency, which is held to be diagnostic of R structure behavior at the heme, had shifted toward the T structure. Moreover, the shift occurred without any evidence of heterogeneity. For the R structure, the ion–histidine frequency is 230 cm^{-1}, whereas for the T structure it drops to 216 cm^{-1}. This

14-cm^{-1} shift corresponds to a reduction in affinity of roughly a factor of 70. However, it is not established whether the shift is linear in the change in affinity. The movement of the marker line by 7 cm^{-1}, which is seen in the cross-linked derivative, represents half the difference between R and T. If the frequency changes were linear in the free energy RT ln c, the cooperative free energy would have been halved, and c thereby increased to 0.3. Thus it is unlikely that the changes are linearly related. Given that the remaining 7 cm^{-1} of lineshift corresponds to roughly the same 70-fold reduction in affinity change between R and T, it is then not unexpected that reducing the affinity of one of the subunits by a mere factor of 5.8 does not show discernible heterogeneity in the line. It could, of course, be argued that the resonance Raman signal responds to enthalpic, rather than entropic, effects and that it is this interplay that is being seen here. On the other hand, changes in the heme pocket geometry may not store much of the cooperative free energy. It would be very interesting to discover the origin of this frequency perturbation in the resonance Raman signal. In the study of Larsen et al. (4), the difference in front face fluorescence upon oxygenation was also observed to change. This has similar calibration problems, in that it is hard to know how energetically significant the changes are that underlie the fluorescence changes.

Further issues

A number of issues remain in explaining the behavior of this cross-linked Hb, particularly the triferric derivative. Fowler et al. (8) found biphasic relaxations in flow or flash, suggestive of R and T rates for ligand rebinding. From the R to T rates determined above, and the low protein and ligand concentrations used by Fowler et al., it is clear that in this case allosteric equilibration will be much more rapid than ligand binding. Therefore, the CO association rates observed must be mixtures of R and T ligand binding rates. Each of the rates observed by Fowler et al. is of the proper order of magnitude, and displays the anticipated sensitivity to the fractional T state, which can be estimated from Marden et al. (21, 22). However, the rapid conversion rates should produce a single apparent rebinding rate in the range observed by Fowler.

This leads to the intriguing question of the origin of the second phase. A solution of the rate equations gives two exponentials, with one being roughly the sum of all the rates. Given our measured values for k_{RT} and k_{TR}, the faster of the two exponentials must have a value far too rapid to be either of the two observed values (and possibly faster than the resolution of the experiment). Interestingly, the CD marker band at 287 nm does not show evidence for the T structure (and also exhibits a different 300-nm shoulder). And, finally, chemical modification studies that are sensitive to quaternary conformation show rates typical of R, rather than T, structures (27). Thus, while the equilibrium and modulation studies show clear and mutually consistent evidence for conversion to the T state, the CD spectra and the presence of additional slow relaxations point to a more complex picture.

We thank Dr. Kim Vandegriff for providing us with her manuscript before publication, and acknowledge helpful suggestions and discussions with Prof. John Olson and Dr. William Eaton.

Received for publication 2 June 1992 and in final form 23 November 1992.

REFERENCES

1. Chatterjee, R., E. V. Welty, R. Y. Walder, S. L. Pruitt, P. H. Rogers, A. Arnone, and J. A. Walder. 1986. Isolation and characterization of a new hemoglobin derivative cross-linked between the å chains (Lysine 99å1-Lysine 99å2). *J. Biol. Chem.* 261:9929–9937.
2. Snyder, S. R., E. V. Welty, R. W. Walder, L. A. Williams, and J. A. Walder. 1987. HbXL99å: a hemoglobin derivative that is cross-linked between the å subunits is useful as a blood substitute. *Proc. Natl. Acad. Sci. USA* 84:7280–7284.
3. Vandegriff, K. D., F. Medina, M. A. Marini, and R. W. Winslow. 1989. Equilibrium and oxygen binding to human hemoglobin cross-linked between the å chains by bis(3,5-dibromosalicyl) fumarate. *J. Biol. Chem.* 264:17824–17833.
4. Larsen, R. W., M. D. Chavez, M. R. Ondrias, S. H. Courtney, J. H. Friedman, M. J. Lin, and R. E. Hirsch. 1990. Dynamics and reactivity of HbXL99å. *J. Biol. Chem.* 265:4449–4454.
5. Vandegriff, K. D., Y. C. LeTellier, R. M. Winslow, R. J. Rohlfs, and J. S. Olson. 1991. Determination of the rate and equilibrium constants for oxygen and carbon monoxide binding to R-state human hemoglobin cross-linked between the å subunits at lysine 99. *J. Biol. Chem.* 266:17049–17059.
6. Ferrone, F. A. 1991. Modulated excitation and structural change in hemoglobin. *Comments Mol. Cell. Biol.* 7:309–332.
7. Martino, A. J., and F. A. Ferrone. 1989. Rate of allosteric change in hemoglobin measured by modulated excition using fluorescence detection. *Biophys. J.* 56:781–794.
8. Fowler, S. A., J. A. Walder, A. DeYoung, L. D. Kwiatkowski, and R. W. Noble. 1992. Isolation and characterization of the triply oxidized derivative of a cross-linked hemoglobin. *Biochemistry.* 31:717–725.
9. Sunshine, H. R., J. Hofrichter, F. A. Ferrone, and W. A. Eaton. 1982. Oxygen binding by sickle cell hemoglobin polymers. *J. Mol. Biol.* 158:251–273.
10. Martino, A. J. 1988. Allosteric kinetics of hemoglobin probed by modulated excitation with fluorescence detection. Ph.D. thesis. Drexel University, Philadelphia, PA.
11. Dolman, D., and S. J. Gill. 1978. Membrane-covered thin-layer optical cell for gas-reaction studies of hemoglobin. *Anal. Biochem.* 87:127–134.
12. Shrager, R. I., and R. W. Hendler. 1982. Titration of individual components in a mixture with resolution of difference spectra, pKs and redox transitions. *Anal. Chem.* 54:1147–1152.

12*a*. Bellelli, A., R. Ippoliti, A. Brancaccio, E. Lendaro, and M. Brunori. 1990. Cooperative ligand binding of crosslinked hemoglobins at very high temperatures. *J. Mol. Biol.* 213:571–574.

13. Zhang, N., F. A. Ferrone, and A. J. Martino. 1990. Allosteric ki-

netics and equilibria differ for carbon monoxide and oxygen binding to hemoglobin. *Biophys. J.* 58:333–340.

14. Shulman, R. G., J. J. Hopfield, and S. Ogawa. 1975. Allosteric interpretation of hemoglobin properties. *Q. Rev. Biophys.* 8:325–420.
15. Eaton, W. A., E. R. Henry, and J. Hofrichter. 1991. Application of linear free energy relations to protein conformational changes: the quaternary structural change of hemoglobin. *Proc. Natl. Acad. Sci. USA* 88:4472–4475.
16. Cho, K. C., and J. J. Hopfield. 1979. Spin equilibrium and quaternary structure change in hemoglobin A. *Biochemistry.* 18:5826–5833.
17. Hofrichter, J., J. H. Sommer, E. R. Henry, and W. A. Eaton. 1983. Nanosecond absorption spectroscopy of hemoglobin: elementary processes in kinetic cooperativity. *Proc. Nat. Acad. Sci. USA* 80:2235–2239.
18. Martin, J., and L. Parkhurst. 1990. A multipass cuvette for laser photolysis studies and its uses in studying hemoglobin kinetics and equilibria. *Anal. Biochem.* 186:288–295.
19. Sawicki, C. A., and Q. H. Gibson. 1976. Quaternary conformational changes in human hemoglobin studied by laser photolysis of carboxyhemoglobin. *J. Biol. Chem.* 251:1533–1542.
20. Szabo, A., and M. Karplus. 1975. Analysis of cooperativity in hemoglobin. Valency hybrids, oxidation and methemoglobin replacement reactions. *Biochemistry.* 14:931–940.
21. Marden, M. C., L. Kiger, J. Kister, B. Bohn, and C. Poyart. 1991. Coupling of ferric iron spin and allosteric equilibrium in hemoglobin. *Biophys. J.* 60:770–776.
22. Marden, M. C., J. Kister, B. Bohn, and C. Poyart. 1991. Allosteric transition in triply met-hemoglobin. *J. Mol. Biol.* 217:303–306.
23. Marden, M. C., J. Kister, C. Poyart, and S. J. Edelstein. 1989. Analysis of hemoglobin oxygen equilibrium curves: are unique solutions possible? *J. Mol. Biol.* 208:341–345.
24. Philo, J. S., and J. W. Lary. 1990. Kinetic investigations of the quaternary enhancement effect and alpha/beta differences in binding the last oxygen to hemoglobin tetramers and dimers. *J. Biol. Chem.*
25. Chu, A. H., B. W. Turner, and G. K. Ackers. 1984. Effects of protons on the oxygenation-linked subunit assembly in human hemoglobin. *Biochemistry.* 23:604–617.
26. Mills, F. C., M. L. Johnson, and G. K. Ackers. 1976. Oxygenation-Linked subunit interactions in human hemoglobin: experimental studies on the concentration dependence of oxygenation curves. *Biochemistry.* 15:5350–5362.
27. Fowler, S. A. 1992. Development of blood substitutes: characterization of chemically modified hemoglobins. Ph.D. thesis. University of Iowa, Ames, IA.
28. Mozzarelli, A., C. Rivetti, G. L., Rossi, E. R. Henry, and W. A. Eaton. 1991. Crystals of haemoglobin with the T quaternary structure bind oxygen noncooperatively with no Bohr effect. *Nature (Lond.).* 351:416–419.
29. Rivetti, C., A. Mozzarelli, G. L. Rossi, E. R. Henry, and W. A. Eaton. 1993. Oxygen binding by single crystals of hemoglobin. *Biochemistry.* In press.
30. Perutz, M. F., J. E. Ladner, S. R. Simon, and C. Ho. 1974. Influence of globin structure on the state of the heme. I. Human deoxyhemoglobin. *Biochemistry.* 13:2163–2173.
31. Ferrone, F. A., A. J. Martino, and S. Basak. 1985. Conformational kinetics of triligated hemoglobin. *Biophys. J.* 48:269–282.
32. Marden, M. C., E. S. Hazard, and Q. H. Gibson. 1986. Testing the two state model: anomalous effector binding to human hemoglobin. *Biochemistry.* 25:7591–7596.
33. Ackers, G. K., and M. L. Johnson. 1981. Linked functions in allosteric proteins. *J. Mol. Biol.* 147:559–582.
34. Imai, K. 1973. Analysis of oxygen equilibria of native and chemically modified human adult hemoglobins on the basis of Adair's stepwise oxygenation theory and the allosteric model of Monod, Wyman and Changeux. *Biochemistry.* 12:798–808.
35. Imai, K., and T. Yonetani. 1975. pH dependence of the Adair constants of human hemoglobin. *J. Biol. Chem.* 250:2227–2231.